Journal of Alloys and Compounds 495 (2010) 561–564

Contents lists available at ScienceDirect

Journal of Alloys and Compounds

journal homepage: www.elsevier.com/locate/jallcom

Retention at room temperature of the tetragonal t″-form in Sc_2O_3-doped ZrO_2 nanopowders

Paula M. Abdala [a,*], Diego G. Lamas [a], Márcia C.A. Fantini [b], Aldo F. Craievich [b]

[a] CINSO (Centro de Investigaciones en Sólidos), CITEFA-CONICET, J.B. de La Salle 4397, 1603 Villa Martelli, Pcia. de Buenos Aires, Argentina
[b] Instituto de Física, FAP, USP, Travessa R da Rua do Matão, No. 187, Cidade Universitaria, 05508-900 São Paulo, Brazil

ARTICLE INFO

Article history:
Received 2 June 2009
Accepted 15 August 2009
Available online 25 August 2009

Keywords:
Nanostructured materials
Oxide materials
Crystal structure
Synchrotron radiation
X-ray diffraction

ABSTRACT

Synchrotron X-ray powder diffraction was applied to the study of the effect of crystallite size on the crystal structure of ZrO_2–10 mol% Sc_2O_3 nanopowders synthesized by a nitrate-lysine gel-combustion route. Nanopowders with different average crystallite sizes were obtained by calcination at several temperatures, ranging from 650 to 1200 °C. The metastable t″-form of the tetragonal phase, exhibiting a cubic unit cell and tetragonal $P4_2/nmc$ spatial symmetry, was retained at room temperature in fine nanocrystalline powders, completely avoiding the presence of the stable rhombohedral β phase. Differently, this phase was identified in samples calcined at high temperatures and its content increased with increasing crystallite size. The critical maximum crystallite size for the retention of the mestastable t″-form resulted of about 35 nm.

1. Introduction

Because of their high ionic conductivity, ZrO_2–Sc_2O_3 ceramics have attracted the attention of many researchers. These materials are promising candidates as solid electrolytes in intermediate-temperature solid-oxide fuel cells (IT-SOFCs). Nevertheless, a decrease in their ionic conductivity after high-temperature treatments is often observed. This effect can be assigned to the developing of certain phases with poor electrical properties. This becomes a key problem for the application of these materials and, for this reason, the equilibrium phase diagram of the ZrO_2–Sc_2O_3 system has been studied by several authors. Although substantial progress has been made in recent years, many uncertainties still remain.

The polymorphs reported for ZrO_2–Sc_2O_3 solid solutions exhibit either monoclinic, tetragonal, cubic or rhombohedral symmetries. The monoclinic and rhombohedral phases exhibit poor electrical properties, while the tetragonal and cubic ones are useful for applications. The existence of rhombohedral phases, such as β, γ and δ, is an important feature of ZrO_2–Sc_2O_3 materials [1,2] and they have not been observed in other ZrO_2-based systems.

Several metastable phases have been found in compositionally homogeneous ZrO_2-based systems. Depending on composition, temperature and crystal size, the tetragonal phase can exhibit three metastable forms named as t, t′ and t″ [2]. The stable tetragonal form is known as the t-form. The t′-form has a wider solubility range, but is unstable in comparison with a mixture of t-form and cubic phase. The t″-form has an axial ratio, c/a, of unity, but its oxygen atoms are displaced along the c-axis from their ideal sites of the cubic phase. Interestingly, the t″-form has not been observed in compositionally homogeneous ZrO_2–Sc_2O_3 solid solutions with large crystallite sizes. Instead, (t′ + β) or (cubic + β) mixtures were found in the range from 9 up to 14 mol% Sc_2O_3 [1].

Yashima and coworkers [2] have proposed a metastable–stable phase diagram for compositionally homogeneous ZrO_2–Sc_2O_3 materials with large grain size, which were synthesized at high temperatures. Differently, the characterization of the phase diagram of nanostructured ZrO_2–Sc_2O_3 solid solutions did not receive much attention up to now. To our knowledge, only Xu et al. [3] have explored some features of the ZrO_2–Sc_2O_3 phase diagram in nanostructured solid solutions. These authors studied the phase transitions in ZrO_2–Sc_2O_3 nanopowders synthesized by a two step hydrothermal process.

In this work, we have investigated the presence and the crystallographic features of the metastable and stable phases exhibited by ZrO_2–10 mol% Sc_2O_3 nanopowders with different average crystallite sizes, ranging from 10 to 140 nm. This study was performed by using synchrotron radiation X-ray powder diffraction (XPD) with a high-intensity setup. The Sc_2O_3 content studied in this work is within the typical compositional range of interest in IT-SOFCs (usually between 7 and 12 mol% Sc_2O_3). For ZrO_2–Sc_2O_3 electrolytes with Sc_2O_3 content close to 10 mol%, operation at temperatures higher than 550 °C is required since at this temperature the β phase transforms to the cubic one. Interestingly, we will demonstrate here

* Corresponding author. Tel.: +54 11 4709 8158; fax: +54 11 4709 8158.
E-mail address: pabdala@citefa.gov.ar (P.M. Abdala).

0925-8388/$ – see front matter © 2009 Elsevier B.V. All rights reserved.
doi:10.1016/j.jallcom.2009.08.083

that the β phase can also be completely suppressed in nanocrystalline solid solutions.

The present work aimed to perform a crystallographic investigation of the metastable phases that are retained at room temperature in nanopowders of ZrO_2–Sc_2O_3 solid solutions with different average crystallite sizes. The phases studied here exist within more or less limited domains of crystallite size, temperature and pressure, very different from those of dense materials used in practical devices. Therefore, in that case, the combined effects of temperature, pressure and average crystallite size must be investigated under real processing conditions. However, the present study provides important new information that could be of technological interest.

2. Experimental

2.1. Synthesis of nanocrystalline ZrO_2–Sc_2O_3 solid solutions

Nanocrystalline ZrO_2–10 mol% Sc_2O_3 powders were obtained by using a recently developed stoichiometric nitrate-lysine gel-combustion process [4]. $ZrO(NO_3)_2{\cdot}6H_2O$ (Alpha Aesar, USA, 99.9%) and $Sc(NO_3)_3{\cdot}4H_2O$ (Standford Materials, USA, 99.99%) were dissolved in distilled water in order to obtain ZrO_2–10 mol% Sc_2O_3. Lysine (Merck, Germany) was added in right stoichiometric proportion for the combustion reaction. The solution was then evaporated and concentrated in a hot plate at 200 °C until a viscous gel was formed. This gel was spontaneously subjected to a vigorous exothermic reaction. The system remained homogeneous during the whole process and no precipitation was observed.

The as-reacted material was firstly heated in air at 650 °C for 2 h in order to remove the carbonaceous residues. Finally, nanopowders with different average crystallite sizes were prepared by calcination in air at different temperatures (850, 935, 1000 or 1200 °C) for 1 h.

2.2. Synchrotron X-ray powder diffraction experiments and data analysis

The crystal structures of the studied nanopowders were determined by synchrotron XPD. These measurements were carried out at the D10B-XPD beamline of the Brazilian Synchrotron Light Laboratory (LNLS, Campinas, Brazil) using a high-intensity and low-resolution configuration, without crystal analyzer [5]. Since the Bragg peaks of nanocrystalline samples are intrinsically broad, the relatively low resolution of the diffractometer configuration does not significantly affect the peak profile. The X-ray wavelength was set at 1.5495 Å.

The average crystallite sizes of the as-synthesized nanopowders, calcined at different temperatures, were determined by means of the Scherrer equation [6].

Rietveld refinements of XPD data were performed by using the program FullProf. By means of this analysis, we have determined the structural parameters and, in the case of mixtures, the weight fraction or abundance of the different component phases.

For the tetragonal phase, we have assumed a $P4_2/nmc$ space group with the cations (Zr^{4+} and Sc^{3+}) and the O^{2-} anions in 2a and 4d positions, respectively. For the cubic phase, the space group was considered to be $Fm\bar{3}m$, with the cations and anions in 4a and 8c positions, respectively. In the case of the rhombohedral β phase, the assigned space group was $R\bar{3}$ with cations and anions in 18f and 6c positions [7], respectively. The peak shape was modeled by a pseudo-Voigt function. The background of each profile was adjusted by using a six-parameter polynomial function in $(2\theta)^n$, $n = 0$–5. Isotropic atomic temperature parameters were used. The thermal parameters corresponding to Zr and Sc atoms were assumed to be equal. The results are reported in terms of the usual pseudo-fluorite unit cell.

The weight fraction of the different phases can be determined from the results of Rietveld refinements by using the following equation:

$$W_i = \sum_{j=1}^{n} \frac{S_i(ZMV)_i}{S_j(ZMV)_j} \quad (1)$$

where W_i is the weight fraction of the phase "i" in a mixture of n phases and S, Z, M and V are the scale factor, the number of basic formula per unit cell, the mass of the formula unit and the unit cell volume, respectively [8].

This quantitative analysis performed by Rietveld refinements was confirmed by using the single line method [9]. This procedure is based on the determination of the ratio between the intensity of a Bragg peak in the mixture I_1 and that of the same peak in a single phase sample I_{1p}. In the present case, we are considering two phases with the same composition and, thus, their respective X-ray mass absorption coefficients are equal. For this simple case, the weight fractions of phases 1 and 2 are given by:

$$W_1 = \frac{I_1}{I_{1p}} \quad \text{and} \quad W_2 = 1 - W_1 \quad (2)$$

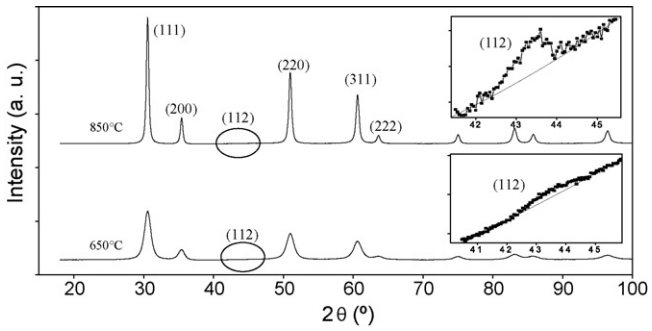

Fig. 1. XPD patterns of ZrO_2–10 mol% Sc_2O_3 powders with average crystallite sizes of 10 nm (below) and 25 nm (above). Insets: Profiles of the (1 1 2) Bragg reflection (forbidden for the cubic phase) associated to the tetragonal t″-form, taken with longer counting times. The increasing trend of the background close to the (1 1 2) Bragg peak is due to a large tail of the strong (2 2 0) Bragg reflection, which is caused by the strong peak broadening of these samples with small average crystallite size.

The discrimination between the cubic phase and the tetragonal t″-form can be achieved through the observation of the (1 1 2) Bragg reflection occurring exclusively in phases of tetragonal symmetry and so forbidden for the cubic one. The (1 1 2) reflection is very weak and is related to small displacements along the c-axis of the O^{2-} anions from their average position in the fluorite-like (cubic) structure. Therefore, the use of a powerful synchrotron X-ray source becomes of critical importance for its detection. The fractional z-coordinate of the O^{2-} anion in the asymmetric unit of the tetragonal unit cell can be calculated from the ratio of the measured integrated intensities of the (1 1 1) and (1 1 2) Bragg peaks, $I(1\,1\,2)$ and $I(1\,1\,1)$, as it was previously demonstrated [5], by applying a simple equation given by:

$$\frac{I(1\,1\,2)}{I(1\,1\,1)} = \frac{4f_0^2 \sin[4\pi z(\mathrm{O})]\, q_0^2 L(1\,1\,2)}{f_{\mathrm{Zr-Sc}}^2 q_{\mathrm{Zr-Sc}}^2 L(1\,1\,1)} \quad (3)$$

where f_0 and q_0 are the scattering factor and the Debye–Waller factor of O^{2-} anions, $f_{\mathrm{Zr-Sc}}$ and $q_{\mathrm{Zr-Sc}}$ are the weighted average of the atomic scattering factor and the Debye–Waller factor of the cations and $L(1\,1\,2)$ and $L(1\,1\,1)$ are the Lorentz factors associated to the (1 1 2) and (1 1 1) Bragg reflections, respectively.

It is deemed that the method based on the application of Eq. (3) is more accurate for the determination of z(O) than Rietveld analysis because the latter simultaneously fits the whole XPD pattern and, therefore, the weight of weak Bragg peaks is underestimated. For this reason, we will only report the results of z(O) obtained from Eq. (3).

3. Results and discussion

The samples with small average crystallite size, up to 25 nm, exhibited the t″-form, while the rhomhohedral β-phase was observed in samples with higher average crystallite size.

XPD patterns corresponding to powders composed of very small crystallites, with average crystallite sizes of 10 and 25 nm are displayed in Fig. 1. The strong reflections can be indexed assuming a fcc (cubic) unit cell. On the other hand, the insets in Fig. 1 indicate the presence of a weak but clearly apparent (1 1 2) Bragg peak, which is forbidden for structures with cubic symmetry. Thus, the crystal structure of these samples can be characterized by a cubic unit cell but with a tetragonal symmetry, demonstrating that it can be identified as the tetragonal t″-form.

Fig. 2 displays the XPD patterns close to the (1 1 1) Bragg reflection of the t″-form for all studied samples, with average crystallite sizes from 10 up to 140 nm. The XPD patterns corresponding to powders with average crystallite sizes of 35 nm or larger indicate the existence of a mixture of tetragonal t″-form (and/or cubic phase) and β phase. The discrimination of the t″-form from the cubic phase could not be achieved for the biphasic samples because the (1 1 2) reflection is masked by others weak reflections of the β phase.

The identified phases, their average crystallite sizes and the t″/cubic content of all the samples are presented in Table 1. It is important to remark that the existence of the t″-form in the ZrO_2–Sc_2O_3 system was not reported in the metastable phase dia-

Table 1
Identified phases, t″/cubic content and crystallite sizes of ZrO_2–10 mol% Sc_2O_3 powders treated at different temperatures. Numbers in parentheses indicate the error in the last significant digit.

Calcination temperature (°C)	Present phase(s)	t″/c content (wt.%)[a]		Average crystallite sizes (nm)	
		Rietveld method	Single line method	t″	β
650	t″	100	100	10(1)	–
850	t″	100	100	25(2)	–
935	t″ (or c) + β[a]	53.4(5)	50(1)	35(3)[b]	35(3)[b]
1000	t″ (or c) + β[a]	24.1(3)	25(1)	50(4)	80(8)
1200	t″ (or c) + β[a]	13.8(2)	13.7(6)	85(8)	$1.4(2) \times 10^2$

[a] It was not possible to differentiate the t″-form and the cubic phase in mixtures with the rhombohedral β phase.
[b] For this sample, the best fitting of XPD data was obtained assuming equal peak broadening for both phases.

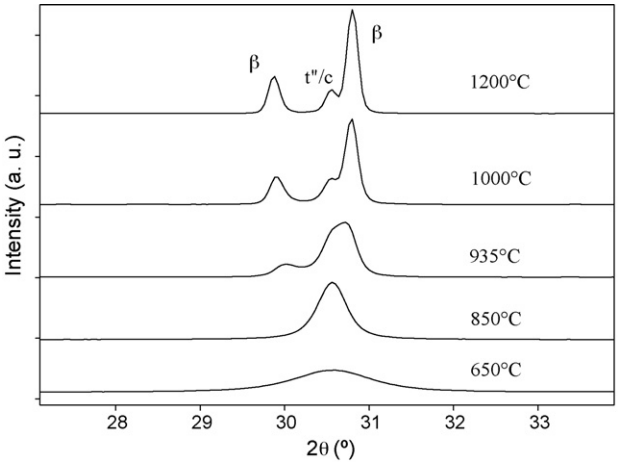

Fig. 2. XPD patterns close to the (1 1 1) most intense Bragg peak corresponding to the t″-form for all the samples studied in this work. The integrated intensities of Bragg peaks corresponding to the β phase increase with increasing average crystallite size (i.e., increasing calcination temperature).

gram proposed by Yashima et al. for compositional homogeneous materials with much larger crystallite sizes [1,2]. We assigned this discrepancy to an effect associated to the nanometric nature of the crystallites in the solid solutions that we have prepared by the gel-combustion process.

It is worth mentioning that the above qualitative analysis of our XPD data is also compatible with the existence of a mixture of the tetragonal t″-form and cubic phase. However, if both phases have different lattice parameter, average crystallite size or microstrain, the profile of the Bragg peaks should be distorted, particularly at high 2θ-angles. The use of a high-intensity synchrotron source made possible a fine study of the peak profile and no evidence of a possible mixture of phases was observed. Rietveld analysis of these samples considering only the tetragonal phase gave excellent agreement factors and confirmed that the axial ratio c/a was equal to 1 within the experimental error for both samples (see Table 2). For these reasons, we assume that these materials were single-phased and only exhibited the t″-form of the tetragonal phase.

The fractional z-coordinate of the O^{2-} anion in the asymmetric unit of the tetragonal unit cell, z(O), determined from the ratio of the integrated intensities of the (1 1 1) and (1 1 2) Bragg peaks (Eq. (3)) resulted of 0.237(2) for both single-phased t″ samples. This value is similar to those reported in the literature for the t″-form in other ZrO_2-based systems [5,10].

The results of Rietveld refinements of our Synchrotron XPD data are summarized in Table 2. As it was mentioned above, the discrimination of the t″-form from the cubic phase could not be achieved, so we have assumed this phase to be cubic in order to simplify the Rietveld refinements of XPD data of biphasic samples. We also assumed that the Debye–Waller factors are equivalent for Zr^{4+} and Sc^{3+} cations and for both phases in order to reduce the number of parameters. The atom positions determined by Wurst et al. for the β phase [7] used in these refinements successfully explained the main and also the weak reflections that appear in the XPD patterns. Rietveld refinements were successfully performed under these hypotheses. Other authors had performed Rietveld analysis assuming 1a and 2c positions [2], but our results based on this model did not fit the observed weak peaks. The lattice parameters derived from our Rietveld refinements resulted in good agreement with those reported in the literature [7].

Both proposed methods for the quantitative analysis gave similar results (see Table 1). The content of the rhombohedral β phase increases with increasing average crystallite size, as expected according the XPD patterns shown in Fig. 2. The sample calcined at 935 °C, with an average crystallite size of 35 nm, contained approximately 50 wt.% of t″-form (and/or cubic phase) and 50 wt.% of β phase. Thus, this crystallite size can be considered as a critical maximum crystallite size for the retention of the t″-form at room

Table 2
Summary of the results obtained from Rietveld refinements of synchrotron XPD data for ZrO_2–10 mol% Sc_2O_3 powders calcined at different temperatures. Numbers in parentheses indicate the error in the last significant digit. Equivalent isotropic Debye–Waller factors were assumed for Zr and Sc. The same Debye–Waller factors were used for both phases.

Calcination temperature (°C)	Space group	Lattice parameters		B(Zr,Sc) (Å^2)	B(O) (Å^2)	R_p	R_{wp}	R_{exp}
		a (Å)	c (Å)					
650	$P4_2/nmc$	5.0878(4)	5.089(1)	1.05(4)	2.4(1)	5.89	7.9	2.46
850	$P4_2/nmc$	5.0887(3)	5.0891(7)	0.99(2)	2.72(7)	6.07	8.01	2.41
935	$Fm\bar{3}m$	5.08864(5)		0.60(3)[a]	1.70(8)[a]	7.33	9.44	2.31
	$R\bar{3}$	19.8531(3)	17.9404(2)					
1000	$Fm\bar{3}m$	5.09284(3)		0.38(3)[a]	1.10(9)[a]	8.48	11.0	2.26
	$R\bar{3}$	19.8244(1)	18.00867(9)					
1200	$Fm\bar{3}m$	5.09189(2)		0.39(9)[a]	0.23(3)[a]	9.1	11.5	2.24
	$R\bar{3}$	19.8153(1)	18.02770(7)					

[a] For the biphasic samples, the Debye–Waller factors of both phases were assumed to be equal.

temperature. For larger crystallite sizes, the content of β phase progressively grows and reaches 86 wt.% of the total volume for the largest crystallite sizes analyzed here. This is consistent with the results reported by Yashima and coworkers for coarse-grained compositionally homogeneous solid solutions [1,2]. The observed transition from the t″-form of the tetragonal phase to a mixture of phases with increasing average crystallite size is probably smeared by the distribution of crystallite sizes and shapes, which were not taken into account in this study.

4. Conclusion

ZrO_2–10 mol% Sc_2O_3 nanopowders with different average crystallite sizes, from 10 up to about 140 nm, were analyzed by synchrotron XPD. We established that the stable rhombohedral β phase can be totally suppressed in nanocrystalline ZrO_2–Sc_2O_3 solid solutions with average crystallite size below a critical maximum size of 35 nm. For this range of average crystallite sizes the t″-form is fully retained at room temperature, thus demonstrating that the phase diagram of ZrO_2–Sc_2O_3 strongly depends on crystallite size. The use of a synchrotron source made possible the detection of very weak XPD reflections of this tetragonal form, allowing us a quantitative determination of the displacement of O^{2-} anions from their ideal positions in the cubic phase.

The presence of the rhombohedral β phase, that coexists with the tetragonal t″-form (and/or the cubic phase), was detected in samples with average crystallite sizes ranging from 35 to 140 nm. Its weight fraction increases with increasing average crystallite sizes, up to a maximum of 85% for the largest average crystallite sizes. These results show that the ZrO_2–10 mol% Sc_2O_3 solid solution gradually tends, for increasing crystallite size, towards the mixture of cubic and rhombohedral phases proposed by Yashima et al. [1] for materials with the same composition and much larger crystallite sizes.

Acknowledgements

This work was supported by the Brazilian Synchrotron Light Laboratory (LNLS, Brazil, proposals D10B-XPD-5364 and 6723), by the scientific collaboration projects CNPq-CONICET and CAPES-SECyT (Brazil–Argentina), CNPq (Brazil, PROSUL program 490289/2005-3), Agencia Nacional de Promoción Científica y Tecnológica (Argentina, PICT 2005 No. 38309 and PICT 2007 No. 01152), CONICET (Argentina, PIP No. 6559) and by Centro Latinoamericano de Física (Latinoamerican Centre of Physics, CLAF). P.M. Abdala thanks CONICET and YPF foundation for her doctoral fellowship.

References

[1] M. Yashima, M. Kakihana, M. Yoshimura, Solid State Ionics 86–88 (1996) 1131–1149.
[2] H. Fujimori, M. Yashima, M. Kakihana, M. Yoshimura, J. Am. Ceram. Soc. 81 (1998) 2885–2893.
[3] G. Xu, Y.W. Zhang, C.S. Liao, C.H. Yan, Phys. Chem. 6 (2004) 5410–5418.
[4] D.G. Lamas, A.M. Rosso, M. Suarez Anzorena, A. Fernández, M.G. Bellino, M.D. Cabezas, N.E. Walsöe de Reca, A.F. Craievich, Scripta Mater. 55 (2006) 553–556.
[5] D.G. Lamas, R.O. Fuentes, I.O. Fábregas, M.E. Fernández de Rapp, G.E. Lascalea, J.R. Casanova, N.E. Walsöe de Reca, A.F. Craievich, J. Appl. Crystallogr. 38 (2005) 867–873.
[6] H. Klug, L. Alexander, X-ray Diffraction Procedures for Polycrystalline and Amorphous Materials, second ed., John Wiley and Sons, New York, 1974.
[7] K. Wurst, E. Schweda, D.J.M. Bevan, J. Mohyla, K.S. Wallwork, M. Hofmann, Solid State Sci. 5 (2003) 1491–1497.
[8] R.A. Young, The Rietveld Method, Oxford University Press, 1993.
[9] D.B. Cullity, Elements of X-ray Diffraction, Addison-Wesley publishing Company Inc, Massachusetts, 1959 (second printing).
[10] M. Yashima, S. Sasaki, M. Kakihana, Y. Yamaguchi, H. Arashi, M. Yoshimura, Acta Crystallogr. B50 (1994) 663–672.